DOI: 10.1534/genetics.107.071100

A Novel Nonnull *ZIP1* Allele Triggers Meiotic Arrest With Synapsed Chromosomes in *Saccharomyces cerevisiae*

Neal Mitra* and G. Shirleen Roeder*,†,‡,[1]

**Department of Molecular, Cellular and Developmental Biology,* †*Howard Hughes Medical Institute and* ‡*Department of Genetics, Yale University, New Haven, Connecticut 06520-8103*

Manuscript received January 17, 2007
Accepted for publication April 6, 2007

ABSTRACT

During meiotic prophase, assembly of the synaptonemal complex (SC) brings homologous chromosomes into close apposition along their lengths. The Zip1 protein is a major building block of the SC in *Saccharomyces cerevisiae*. In the absence of Zip1, SC fails to form, cells arrest or delay in meiotic prophase (depending on strain background), and crossing over is reduced. We created a novel allele of *ZIP1*, *zip1-4LA*, in which four leucine residues in the central coiled-coil domain have been replaced by alanines. In the *zip1-4LA* mutant, apparently normal SC assembles with wild-type kinetics; however, crossing over is delayed and decreased compared to wild type. The *zip1-4LA* mutant undergoes strong checkpoint-induced arrest in meiotic prophase; the defect in cell cycle progression is even more severe than that of the *zip1* null mutant. When the *zip1-4LA* mutation is combined with the *pch2* checkpoint mutation, cells sporulate with wild-type efficiency and crossing over occurs at wild-type levels. This result suggests that the *zip1-4LA* defect in recombination is an indirect consequence of cell cycle arrest. Previous studies have suggested that the Pch2 protein acts in a checkpoint pathway that monitors chromosome synapsis. We hypothesize that the *zip1-4LA* mutant assembles aberrant SC that triggers the synapsis checkpoint.

THE synaptonemal complex (SC) is a proteinaceous structure found along the lengths of homologous chromosomes during the pachytene stage of meiotic prophase. This elaborate structure, which is morphologically conserved across many eukaryotic species, holds homologous chromosomes in close proximity along their lengths (reviewed by Zickler and Kleckner 1999). Each SC consists of two lateral elements, corresponding to the proteinaceous cores of the individual chromosomes within the complex, separated by an intervening central region.

Another hallmark of meiotic prophase is meiotic recombination. This process is initiated by DNA double-strand breaks created by the topoisomerase II-like Spo11 protein (reviewed by Keeney 2001). After double-strand breaks are formed, a series of protein-catalyzed steps leads to the creation of two types of recombinants, crossovers and noncrossovers (Allers and Lichten 2001). Crossovers give rise to chromatin bridges between homologs that ensure their correct segregation at the first meiotic division. Failure to cross over can lead to nondisjunction and consequent inviability of meiotic products.

In budding yeast, recombination and chromosome synapsis are concurrent events (Padmore *et al.* 1991; Schwacha and Kleckner 1994). Double-strand breaks appear prior to the formation of mature SC. Joint molecules (Holliday junctions) are present when the SC is fully formed, and mature recombinants are produced around the time that the SC disassembles. Synapsis is not required for the initiation of recombination, but steps in the recombination pathway appear to be required for synapsis (reviewed by Roeder 1997; Zickler and Kleckner 1999).

In *Saccharomyces cerevisiae*, Zip1 is a component of the central region of the SC (Sym *et al.* 1993). Zip1 is an 875-amino-acid protein with a predicted, α-helical coiled-coil domain flanked by globular domains. Zip1 forms a homodimer with the two proteins oriented in register; a pair of dimers lies head to head to span the space between lateral elements (Dong and Roeder 2000). The *zip1* null mutation (herein referred to as *zip1*Δ) exhibits defects in chromosome synapsis, with chromosomes homologously paired, but not intimately synapsed. In the absence of Zip1, the cores of each pair of homologous chromosomes are closely associated at only a few sites (Sym *et al.* 1993), presumed to be the sites at which synapsis normally initiates (Chua and Roeder 1998; Fung *et al.* 2004). The *zip1*Δ mutant exhibits an approximately threefold decrease in meiotic crossing over compared to wild type, with the magnitude of the effect varying from interval to interval (Sym *et al.* 1993; Sym and Roeder 1994; Storlazzi *et al.* 1996).

During meiosis, a checkpoint mechanism arrests cells in midmeiotic prophase in response to defects in

[1]*Corresponding author:* Department of Molecular, Cellular and Developmental Biology, Yale University, P.O. Box 208103, New Haven, CT 06520-8103. E-mail: shirleen.roeder@yale.edu

recombination (reviewed by Bailis and Roeder 2000). Mutants that accumulate unrepaired breaks with single-stranded tails (*e.g.*, *dmc1* and *hop2*) trigger the checkpoint and undergo delay or arrest in prophase (Bishop *et al.* 1992; Rockmill *et al.* 1995; Leu *et al.* 1998). Introduction of a *spo11* mutation into these mutant backgrounds alleviates the arrest by preventing the initiation of recombination and the consequent accumulation of recombination intermediates (Bishop *et al.* 1992; Leu *et al.* 1998). Arrest can also be alleviated by mutations in the *DDC1*, *MEC3*, and *RAD17* genes (Lydall *et al.* 1996; Thompson and Stahl 1999; Hong and Roeder 2002), whose products are involved in sensing DNA damage, such as unrepaired double-strand breaks (reviewed by Zhou and Elledge 2000).

Downstream targets of the checkpoint include Swe1 and Ndt80. During checkpoint activation, the Swe1 kinase accumulates and becomes hyperphosphorylated (Leu and Roeder 1999) and in turn phosphorylates Cdc28. This phosphorylation negatively regulates Cdc28 and limits the activity of the cyclin-dependent kinase complex Cdc28-Clb1 (Booher *et al.* 1993), whose activity is required for the exit from pachytene (Shuster and Byers 1989). Ndt80 is a meiotic transcription factor that activates genes required for exit from pachytene, including Clb1 (Chu and Herskowitz 1998; Hepworth *et al.* 1998). Activation of the pachytene checkpoint prevents the accumulation and Ime2-dependent phosphorylation of Ndt80 (Tung *et al.* 2000; Benjamin *et al.* 2003), thereby inhibiting Ndt80 activity.

Mutation of the meiosis-specific checkpoint *PCH2* gene was identified on the basis of its ability to bypass the sporulation defect of the *zip1*Δ mutant (San-Segundo and Roeder 1999). Unlike the *ddc1*, *mec3*, and *rad17* mutations, *pch2* does not bypass the *hop2* mutant arrest and has little or no effect on sporulation in the *dmc1* mutant (San-Segundo and Roeder 1999; Zierhut *et al.* 2004; Hochwagen *et al.* 2005). Thus, its effect seems to be relatively specific for *zip1*. Studies in *Caenorhabditis elegans*, an organism in which synapsis is not dependent on recombination, revealed a checkpoint that specifically monitors chromosome synapsis, independently of a DNA-damage checkpoint (Bhalla and Dernburg 2005). This synapsis checkpoint requires the *C. elegans* homolog of *PCH2*. Recent studies led Wu and Burgess (2006) to propose that a Pch2-dependent synapsis checkpoint also operates in budding yeast.

We have generated and characterized a novel allele of the *S. cerevisiae ZIP1* gene. This mutation, called *zip1-4LA*, results from changing four leucine residues in the coiled-coil region to alanines. This mutant makes SC with normal kinetics, but it nevertheless undergoes arrest at pachytene. Thus, *zip1-4LA* appears to uncouple the synapsis and sporulation functions of Zip1. The *zip1-4LA* mutant phenotype is fully suppressed by the *pch2* mutation, leading us to propose that *zip1-4LA* makes an aberrant SC that triggers the synapsis checkpoint.

MATERIALS AND METHODS

Genetic methods and strains: Yeast manipulations were carried out using standard procedures (Sherman *et al.* 1986). Genotypes of relevant strains are presented in Table 1. Diploids were made by mating appropriate haploids, generated by transformation and/or genetic crosses.

The following gene deletion/disruption constructs were described previously: pML54 for *mec3::TRP1* (Longhese *et al.* 1996), pTP89 for *ndt80::LEU2* (Tung *et al.* 2000), pSS52 for *pch2::URA3* (San-Segundo and Roeder 1999), pDL183 for *rad17::LEU2* (Lydall and Weinert 1997), pME302 for *spo11::ADE2* (Engebrecht and Roeder 1989), p(spo13)16 for *spo13::URA3* (Wang *et al.* 1987), pMB97 for *zip1::LEU2* (Sym *et al.* 1993), pMB116 for *zip1::LYS2* (Sym and Roeder 1994), and pMB117 for *zip1::URA3* (Sym and Roeder 1995).

The *ddc1::ADE2* disruption plasmid pB219 was created by Beth Rockmill as follows. The *Sph*I–*Bam*HI fragment of *DDC1* was cloned between the *Sph*I and *Bam*HI sites of the SK+ plasmid (Stratagene, Cedar Creek, TX) to yield pB215. The *Sma*I–*Pst*I fragment of *ADE2* was then subcloned into pB215 between the *Hpa*I and *Pst*I sites to yield pB219, which was then cut with *Xma*I and *Sph*I for targeting gene disruption in yeast. The *zip1::KanMX4*, *swe1::KanMX4*, and *pch2::HphMX4* disruptions were created by transformation with PCR products derived from the *KanMX4* and *HphMX4* drug resistance cassettes (Wach *et al.* 1994; Goldstein and McCusker 1999). For *zip1::KanMX4* and *pch2::HphMX4*, primers extending 40 nucleotides inward from the start and stop codons of *ZIP1* and *PCH2* were used to delete almost all of the coding sequence of each gene. For *swe1::KanMX4*, primers complementary to untranslated regions flanking *SWE1* were used such that the entire gene was deleted.

In-frame deletions of *ZIP1* and *zip1-4LA*: In-frame deletions of *ZIP1* were created by PCR amplification of plasmid pHD 130(T7), which consists of the *ZIP1 Hin*cII–*Hin*cII fragment (nucleotides 1534–2472) inserted into the unique *Sma*I site of pQE30(T7). The pQE30(T7) plasmid is a modified version of pQE30 (QIAGEN, Valencia, CA) in which the nucleotides between the *Xho*I and *Eco*RI sites flanking the T5 promoter were replaced with a T7 promoter and *lac* operator sequence specified by the following oligonucleotide: 5′-CTCGAGAAA TTAATACGACTCACTATAGGCCTGGAATTGTGAGCGGATA ACAATTCCGAATTC-3′. For each deletion, 5′-phosphorylated primers oriented outward from the site of the intended deletion were used to amplify ~4.4 kb of DNA, which was then circularized by T4 DNA Ligase (New England Biolabs, Ipswich, MA). Template DNA was degraded using *Dpn*I (New England Biolabs). To ensure fidelity of replication, Pfu Turbo DNA polymerase (Stratagene, La Jolla, CA) was used; the resulting plasmids were confirmed by DNA sequencing.

Deletion constructs were then transferred into the context of full-length *ZIP1* as follows. The pRS315 vector (Sikorski and Hieter 1989) was modified to create plasmid pRS315-EPN by replacing the nucleotide sequence between *Eag*I and *Xho*I with an oligonucleotide containing *Eag*I, *Pst*I, and *Nhe*I sites but no *Xho*I site: 5′-CGGCCGAACTGCAGAAGCGAGC TAGCAAGTCGAG-3′. Full-length *ZIP1* and flanking sequence were removed from plasmid pMB96 (Sym *et al.* 1993) by digestion with *Pst*I and *Xba*I and inserted into pRS315-EPN between the *Pst*I and *Nhe*I sites, thus destroying both the *Nhe*I and *Xba*I sites and creating pRS315-EPN-Zip1. Three restriction sites (that do not alter the encoded amino acids) were introduced into the 3′ end of *ZIP1* at positions 2389 (*Xba*I), 2478 (*Ava*I), and 2592 (*Hin*dIII) using overlap PCR (Ho *et al.* 1989) to create pRS315-EPN-Zip1(mut). The deletion constructs were transferred into pRS315-EPN-Zip1(mut) by gap repair (Oldenburg *et al.* 1997). A gap of 23 bp was created by

TABLE 1

Yeast strains used in this study

Strain	Genotype	Background
BR2495[a]	$\frac{MAT\mathbf{a}\ \ leu2\text{-}27\ \ his4\text{-}280\ \ arg4\text{-}8\ thr1\text{-}1\ \ ade2\text{-}1}{MAT\alpha\ leu2\text{-}3,112\ his4\text{-}260\ \ ARG4\ thr1\text{-}4\ \ ade2\text{-}1}$ $\frac{ura3\text{-}1\ \ trp1\text{-}1\ \ CYH10}{ura3\text{-}1\ \ trp1\text{-}289\ \ cyh10}$	BR2495
MY152[b]	BR2495 but homozygous *zip1::URA3*	BR2495
NMY101	MY152 plus pRS315-zip1ΔB	BR2495
NMY102	MY152 plus pRS315-zip1ΔC	BR2495
NMY103	MY152 plus pRS315-zip1ΔD	BR2495
NMY104	MY152 plus pRS315-zip1ΔE	BR2495
NMY105	MY152 plus pRS315-zip1ΔF	BR2495
NMY106	MY152 plus pRS315-zip1ΔG	BR2495
NMY107	MY152 plus pRS315-zip1ΔH	BR2495
NMY109	MY152 plus pRS315-zip1ΔJ	BR2495
NMY111	MY152 plus pRS315-ZIP1	BR2495
NMY112	MY152 plus pRS315-zip1-4LA	BR2495
NMY113	MY152 plus pRS315	BR2495
NMY276	MY152 plus pRS315-zip1-L643A	BR2495
NMY278	MY152 plus pRS315-zip1-L650A	BR2495
NMY280	MY152 plus pRS315-zip1-L657A	BR2495
NMY282	MY152 plus pRS315-zip1-L664A	BR2495
NMY274[c]	$\frac{MAT\mathbf{a}\ leu2\text{-}3,112\ his4\text{-}260\ \ ARG4\ thr1\text{-}4\ \ ade2\text{-}1}{MAT\alpha\ leu2\text{-}3,112\ his4\text{-}260\ \ ARG4\ thr1\text{-}4\ \ ade2\text{-}1}$ $\frac{ura3\text{-}1\ \ trp1\text{-}289}{ura3\text{-}1\ \ trp1\text{-}289}$	BR1919-8B 2n
NMY363	NMY274 but homozygous *zip1-4LA*	BR1919-8B 2n
NMY364	NMY274 but homozygous *zip1::URA3*	BR1919-8B 2n
NMY233	NMY *274* but $\frac{zip1\text{-}4LA}{ZIP1}$	BR1919-8B 2n
NMY533	NMY274 but homozygous *ndt80::LEU2 zip1-4LA*	BR1919-8B 2n
NMY539	NMY274 but homozygous *ndt80::LEU2*	BR1919-8B 2n
NMY385	NMY274 but homozygous *spo11::ADE2 zip1-4LA*	BR1919-8B 2n
NMY422	NMY274 but homozygous *spo11::ADE2*	BR1919-8B 2n
NMY602	NMY274 but homozygous *rad17::LEU2 zip1-4LA*	BR1919-8B 2n
NMY605	NMY274 but homozygous *rad17::LEU2 zip1::URA3*	BR1919-8B 2n
NMY608	NMY274 but homozygous *rad17::LEU2*	BR1919-8B 2n
NMY611	NMY274 but homozygous *ddc1::ADE2 zip1-4LA*	BR1919-8B 2n
NMY614	NMY274 but homozygous *ddc1::ADE2 zip1::URA3*	BR1919-8B 2n
NMY617	NMY274 but homozygous *ddc1::ADE2*	BR1919-8B 2n
NMY644	NMY274 but homozygous *mec3::TRP1 zip1-4LA*	BR1919-8B 2n
NMY647	NMY274 but homozygous *mec3::TRP1 zip1::URA3*	BR1919-8B 2n
NMY641	NMY274 but homozygous *mec3::TRP1*	BR1919-8B 2n
NMY340	NMY274 but homozygous *swe1::KanMX4 zip1-4LA*	BR1919-8B 2n
NMY345	NMY274 but homozygous *swe1::KanMX4 zip1::URA3*	BR1919-8B 2n
NMY432	NMY274 but homozygous *swe1::KanMX4*	BR1919-8B 2n
NMY650[d]	$\frac{HIS4\ \ leu2\text{-}3,112\ MAT\mathbf{a}\ \ arg4\text{-}Bgl\ THR1}{his4\text{-}260\ \ LEU2\ \ MAT\alpha\ iADE2\ \ ARG4\ thr1\text{-}4}$ $\frac{ade2\text{-}1\ \ ura3\text{-}1\ \ trp1\text{-}289}{ade2\text{-}1\ \ ura3\text{-}1\ \ trp1\text{-}289}$	BR1919-8B 2n
NMY661	NMY650 but homozygous *pch2::HphMX4 zip1-4LA*	BR1919-8B 2n
NMY664	NMY650 but homozygous *pch2::HphMX4 zip1::KanMX4*	BR1919-8B 2n
NMY654	NMY650 but homozygous *pch2::HphMX4*	BR1919-8B 2n
NMY562	NMY274 but homozygous *swe1::KanMX4 pch2::URA3 zip1-4LA*	BR1919-8B 2n
NMY559	NMY274 but homozygous *swe1::KanMX4 pch2::URA3 zip1::LYS2*	BR1919-8B 2n
NMY565	NMY274 but homozygous *swe1::KanMX4 pch2::URA3*	BR1919-8B 2n
NMY268[e]	NMY274 but *MAT*α-bearing chromosome III is circular and $\frac{spo13::URA3}{SPO13}$	BR1919-8B 2n

(*continued*)

TABLE 1

(Continued)

Strain	Genotype	Background
NMY270	NMY*268* but $\frac{zip1::LYS2}{zip1::KanMX4}$	BR1919-8B 2n
NMY272	NMY*268* but $\frac{zip1\text{-}4LA}{zip1::KanMX4}$	BR1919-8B 2n
NMY671	NMY*268* but $\frac{pch2::HphMX4}{pch2::HphMX4}\ \frac{ZIP1}{zip1::KanMX4}$	BR1919-8B 2n
NMY672	NMY268 but homozygous *pch2-HphMX4 zip1-KanMX4*	BR1919-8B 2n
NMY673	NMY*268* but $\frac{pch2::HphMX4}{pch2::HphMX4}\ \frac{zip1\text{-}4LA}{zip1::KanMX4}$	BR1919-8B 2n
NMY471[f]	NMY274 but *MAT*α-bearing chromosome III is circular and congenic with $\frac{swe1::KanMX4}{swe1::KanMX4}\ \frac{ZIP1}{zip1::LEU2}$	BR1919-8B 2n
NMY472[f]	NMY274 but *MAT*α-bearing chromosome III is circular and congenic with $\frac{swe1::KanMX4}{swe1::KanMX4}\ \frac{zip1\text{-}4LA}{zip1::LEU2}$	BR1919-8B 2n
NMY473[f]	NMY274 but *MAT*α-bearing chromosome III is circular and congenic with $\frac{swe1::KanMX4}{swe1::KanMX4}\ \frac{zip1::URA3}{zip1::LEU2}$	BR1919-8B 2n
NMY401	NMY274 but homozygous *zip1-ΔC*	BR1919-8B 2n
NMY402	NMY274 but homozygous *zip1-ΔD*	BR1919-8B 2n
NMY403	NMY274 but homozygous *zip1-ΔE*	BR1919-8B 2n
NMY404	NMY274 but homozygous *zip1-ΔF*	BR1919-8B 2n
NMY405	NMY274 but homozygous *zip1-ΔJ*	BR1919-8B 2n
NMY461[g]	$\frac{MAT\mathbf{a}\ leu2\ lys2\ ho\text{-}lys2\ trp1\ zip1\text{-}LYS2}{MAT\alpha\ leu2\ lys2\ ho\text{-}lys2\ trp1\ zip1\text{-}LYS2}$ $\frac{pRS306\text{-}ZIP1@URA3}{pRS306\text{-}ZIP1@URA3}$	SK1
NMY462[g]	$\frac{MAT\mathbf{a}\ leu2}{MAT\alpha\ leu2}\ \frac{lys2}{lys2}\ \frac{ho\text{-}lys2\ trp1\ zip1\text{-}LYS2}{ho\text{-}lys2\ trp1\ zip1\text{-}LYS2}$ $\frac{pRS306\text{-}zip1\text{-}4LA@URA3}{pRS306\text{-}zip1\text{-}4LA@URA3}$	SK1
NMY463[g]	$\frac{MAT\mathbf{a}\ leu2}{MAT\alpha\ leu2}\ \frac{lys2}{lys2}\ \frac{ho\text{-}lys2\ trp1\ zip1\text{-}LYS2}{ho\text{-}lys2\ trp1\ zip1\text{-}LYS2}\ \frac{pRS306@URA3}{pRS306@URA3}$	SK1

[a] BR2495 was described by Rockmill and Roeder (1990). The *MAT*α parent of BR2495 is BR1919-8B (Rockmill and Roeder 1990).

[b] MY152 was described by Sym and Roeder (1995).

[c] NMY274 is a diploid strain whose *MAT*α haploid parent is isogenic with BR1919-8B (Rockmill and Roeder 1990) and whose *MAT***a** haploid parent was generated by switching the mating type of BR1919-8B (Rockmill *et al.* 1995).

[d] NMY650 is isogenic with NMY274 except for the markers noted, including a copy of *ADE2* inserted at an ectopic location on chromosome III (designated *iADE2*).

[e] NMY268 is a diploid consisting of a *MAT*α strain isogenic with BR1919-8B that carries a circular version of chromosome III and is *spo13::URA3* mated to *MAT***a** BR1919-8B.

[f] NMY471–NMY473 are diploids consisting of a *MAT*α strain congenic with BR1919-8B that carries a circular version of chromosome III and is *swe1::KanMX4 zip1::LEU2* mated to *MAT***a** BR1919-8B strains that are *swe1::KanMX4* and *ZIP1* (NMY471) or *zip1-4LA* (NMY472) or zip1*::URA3* (NMY473).

[g] NMY461–NMY463 are isogenic with SK1 (Alani *et al.* 1987).

digestion with *Bsu*36I (2365) and *Xba*I (2389). The digested plasmid was cotransformed into MY152 with PCR products (corresponding to *ZIP1* nucleotides 1534–2472) amplified from the pQE(T7) plasmids containing each deletion. The resulting constructs are shown in Figure 1A and the corresponding strains are NMY101–NMY109. Strains NMY111 and NMY113 were used as positive and negative controls, respectively. Deletion constructs *zip1-ΔC*, *zip1-ΔD*, *zip1-ΔE*, *zip1-ΔF*, and *zip1-ΔJ* were substituted into the genome in the same manner as *zip1-4LA* (see below) to yield strains NMY401–NMY405.

For the creation of *zip1-4LA*, site-directed mutagenesis was performed on pRS315-EPN-Zip1(mut) using overlap PCR (Ho *et al.* 1989) to replace the codons for leucine with those for alanine at the appropriate positions (L643A, L650A, L657A, and L664A). The resulting plasmid was transformed into MY152 to yield NMY112. To substitute *zip1-4LA* into the genome, a *MAT*α BR1919-8B *zip1::URA3* haploid strain was transformed with linear, double-stranded DNA containing the full-length *zip1-4LA* gene and transformants were selected on 5-FOA (Toronto Research Chemicals, Toronto) to select for loss of the *URA3* marker (Boeke *et al.* 1984). A correct transformant was then crossed to a wild-type BR1919-8B *MAT***a** strain to derive a *zip1-4LA* strain of the opposite mating type. Two *zip1-4LA* BR1919-8B-derived haploids of opposite mating type were then mated, resulting in strain NMY363.

To assess the presence of the *zip1-4LA* allele in meiotic products of heterozygous diploids, primers specific to *zip1-4LA*, nucleotides 1950–1970 (5′-GAAGGCTCATGAATTG GAGGC-3′) and to the 3′ end of *ZIP1*, nucleotides 2606–2628 (5′-CTATTTCCTTCTCCTTTTCTTGC-3′) were used. These primers generate a PCR product of 679 bp, diagnostic of the presence of *zip1-4LA*. Wild-type *ZIP1* is not amplified.

To integrate *zip1-4LA* into SK1, the full-length *zip1-4LA* gene was subcloned into pRS306 (Sikorski and Hieter 1989) between the *Sac*II and *Kpn*I sites and then integrated at the *URA3* locus (targeted using *Bsm*I) of haploid *zip1::LYS2* SK1 strains. The strains were then mated, resulting in strain NMY462. Control strains were likewise created, using *ZIP1* subcloned into pRS306 at the same sites (NMY461) or using an empty pRS306 vector (NMY463).

To create *zip1-L643A*, *zip1-L650A*, *zip1-L657A*, and *zip1-L664A*, pRS315-EPN-Zip1 was modified as follows. The *Pst*I site was destroyed by digestion with *Pst*I, followed by treatment with the large Klenow fragment of DNA polymerase I (New England Biolabs) to remove the 3′ overhangs. The vector was recircularized by T4 DNA Ligase (New England Biolabs) to yield pRS315-EN-Zip1. Next, three restriction sites that do not alter the encoded amino acids were introduced at *ZIP1* positions 1918 (*Pst*I), 2001 (*Xba*I), and 2107 (*Hin*dIII), using overlap PCR (Ho *et al.* 1989). For each point mutant, the sequence between the *Pst*I and *Xba*I sites in pRS315-EN-Zip1 was replaced by a double-stranded oligonucleotide with appropriate overhanging ends, generated by annealing complementary oligonucleotides containing the required codon. The resulting plasmids were transformed into a BR2495 strain in which *ZIP1* was deleted, resulting in strains NMY276, NMY278, NMY280, and NMY282.

Sporulation and spore viability: Sporulation was performed at 30° in liquid sporulation medium (SPM) (2% potassium acetate, pH 7.0) for nuclear division assays, for spreads of meiotic nuclei, and for physical recombination assays. All other sporulation was performed on SPM in agar plates at 30° for 2 days. The dityrosine assay (Esposito *et al.* 1991) was used to assay the presence or absence of spores for *zip1* deletion mutants. Yeast spore walls include a macromolecule containing dityrosine, which fluoresces under UV light. Patches of cells were placed on top of a nitrocellulose filter on SPM plates and allowed to sporulate for 2 days. Fluorescence was viewed with a UV light source (302 nm) and photographed through a blue Wratten 47b gelatin filter (Kodak, Rochester, NY). For quantification of sporulation, at least 200 cells for each strain were assayed by phase-contrast microscopy for each experiment; every experiment was performed in triplicate.

Spore viability was determined by tetrad dissection. The numbers of spores scored were 880 for wild type, 1144 for *pch2*, 1144 for *pch2 zip1-4LA*, 2640 for *pch2 zip1*, and 176 each for all other strains analyzed for viability.

Cytology: To determine the kinetics of meiotic nuclear division, cells were fixed in 50% ethanol and frozen at −20° prior to staining with 4′,6-diamidino-2-phenylindole (DAPI) (Hong and Roeder 2002). Cells were visually scored using a fluorescence microscope (Nikon E800, see below). For each experiment, at least 100 nuclei per strain per time point were scored. Each experiment was performed three times.

Spread meiotic nuclei were prepared and stained with antibodies as described by Dresser and Giroux (1988). Chromosomal DNA was visualized by staining with DAPI. For Figure 2B, affinity-purified, mouse polyclonal anti-Zip1 antibody (Chua and Roeder 1998) was used at 1:100 dilution, and rabbit polyclonal anti-Red1 antiserum (Smith and Roeder 1997) was used at 1:400 dilution. Donkey anti-mouse antibody conjugated to FITC and donkey anti-rabbit antibody conjugated to Texas Red were used at 1:200 dilution (both from Jackson ImmunoResearch Labs, West Grove, PA). For Figure 3A, affinity-purified, rabbit polyclonal anti-Zip1 antibody (Sym *et al.* 1993) was used at 1:50 dilution, and rat anti-tubulin antibody (Sera-Lab, West Sussex, UK) was used at 1:400 dilution. Donkey anti-rabbit antibody conjugated to Texas Red and donkey anti-rat antibody conjugated to FITC (both from Jackson ImmunoResearch Labs) were used at 1:200 dilution.

A Nikon E800 microscope, equipped with a 100× Plan Apo objective lens, epifluorescence optics, and a Chroma 86012 filter set (Micro Video Instruments, Avon, MA), was used to observe antibody-stained meiotic chromosomes. Images were captured by a Photometrics Cool Snap HQ CCD camera and processed with IPLab Spectrum software v.3.9.5r2 (BD Bioscience, Franklin Lakes, NJ).

For the time-course experiment to monitor the kinetics of SC formation (Figure 3), multiple nuclear spreads were photographed in one field of view and then scored individually. Nine different time points were assayed in each of two independent experiments. At each time point, at least 100 nuclear spreads were scored for each strain, NMY533 and NMY539. The total numbers of spreads scored were 2614 for experiment A and 1966 for experiment B. The results of the two experiments were qualitatively similar, and the data for experiment B are presented in Figure 3B.

Physical recombination assays: The assays were performed as previously described by Tsubouchi *et al.* (2006). Briefly, Southern blot analysis was carried out using a radiolabeled probe for chromosome III, prepared as described by Agarwal and Roeder (2000). Blots were visualized and crossover products were quantified by phosphorimaging in a Storm 860 Gel and Blot Imaging System and using ImageQuant software (GE Healthcare Bio-Sciences, Piscataway, NJ). Physical assays were performed at least three times for each experiment, and the results obtained were qualitatively similar.

Genetic analysis: Crossover frequencies were determined by tetrad dissection for four intervals (chromosome III, *HIS4-LEU2*, *LEU2-MAT*, *MAT-ADE2*; chromosome VIII, *ARG4-THR1*). The numbers of tetrads dissected were 220 for wild type, 286 for *pch2*, 286 for *pch2 zip1-4LA*, and 660 for *pch2 zip1*. Distributions of tetrad types (parental ditype, nonparental ditype, tetratype) were compared using the *G*-test of homogeneity (*e.g.*, Sokal and Rohlf 1995), using a Microsoft Excel

calculator created by Ed Louis and Faiz Abdullah, to assess statistical differences among the four strains.

RESULTS

Deletion analysis of *ZIP1*: Previous deletion analysis of *ZIP1* revealed that deletions of amino acid residues 409–700 (*zip1-M2*) and 409–799 (*zip1-MC1*), affecting the coiled-coil region, cause cells to arrest at pachytene (Tung and Roeder 1998). To narrow further the region within the coiled coil responsible for cell cycle arrest, seven smaller in-frame deletions of 34 codons each were created (Figure 1A), inserted into a centromere-containing plasmid, and introduced into a BR2495 strain background in which the *ZIP1* gene is deleted. Strains carrying these *zip1* deletion constructs were examined for sporulation by a dityrosine assay (Esposito *et al.* 1991). (Yeast spore walls include a macromolecule containing dityrosine, which fluoresces under UV light.) *zip1*-Δ*D* (Δ621–654) and *zip1*-Δ*E* (Δ655–688) each cause sporulation arrest, whereas constructs with deletions immediately upstream (ΔB and ΔC) and downstream (ΔF and ΔG) of regions D and E do not trigger arrest. A smaller deletion of 22 residues, *zip1*-Δ*J* (Δ643–664), was created that partially overlaps both regions D and E. The *zip1*-Δ*J* mutant also arrests.

Examination of the Zip1 amino acid sequence in regions D–F reveals a motif resembling a leucine zipper, although there is no adjacent stretch of basic residues as observed in the canonical leucine zipper motif (Landschulz *et al.* 1988; Alber 1992). When an α-helical wheel is plotted for Zip1 residues 640–723 (approximately regions D–F), it is evident that leucines are present at position d of the helix in many cases (Figure 1B). A new mutant was constructed in which the four leucines at position d within region J were replaced by alanines. The mutant, called *zip1-4LA* (L643A, L650A, L657A, L664A), was assayed for sporulation by phase-contrast microscopy; *zip1-4LA* is unable to sporulate in the BR2495 strain background.

The *zip1*Δ mutant is unable to sporulate in BR2495, but it is able to sporulate at low levels (~5%) in the BR1919-8B diploid strain background (B. Rockmill, personal communication). To examine the effect of *zip1-4LA* in this background, a BR1919-8B diploid homozygous for *zip1-4LA* (substituted for the wild-type *ZIP1* gene on the chromosome) was constructed and analyzed. Surprisingly, even in this strain background, *zip1-4LA* (NMY363) completely fails to sporulate, demonstrating that *zip1-4LA* causes a tighter arrest than the *zip1*Δ mutant (NMY364). In the SK1 strain background, *zip1*Δ does sporulate, after a delay and with reduced efficiency (Sym and Roeder 1994; Storlazzi *et al.* 1996; Xu *et al.* 1997). The *zip1-4LA* mutant sporulates less efficiently than *zip1*Δ in SK1: 30.9% for *zip1-4LA* (NMY462) *vs.* 48.5% for *zip1*Δ (NMY463) and 94.8% for wild type (NMY461). Using the homogeneity chi-

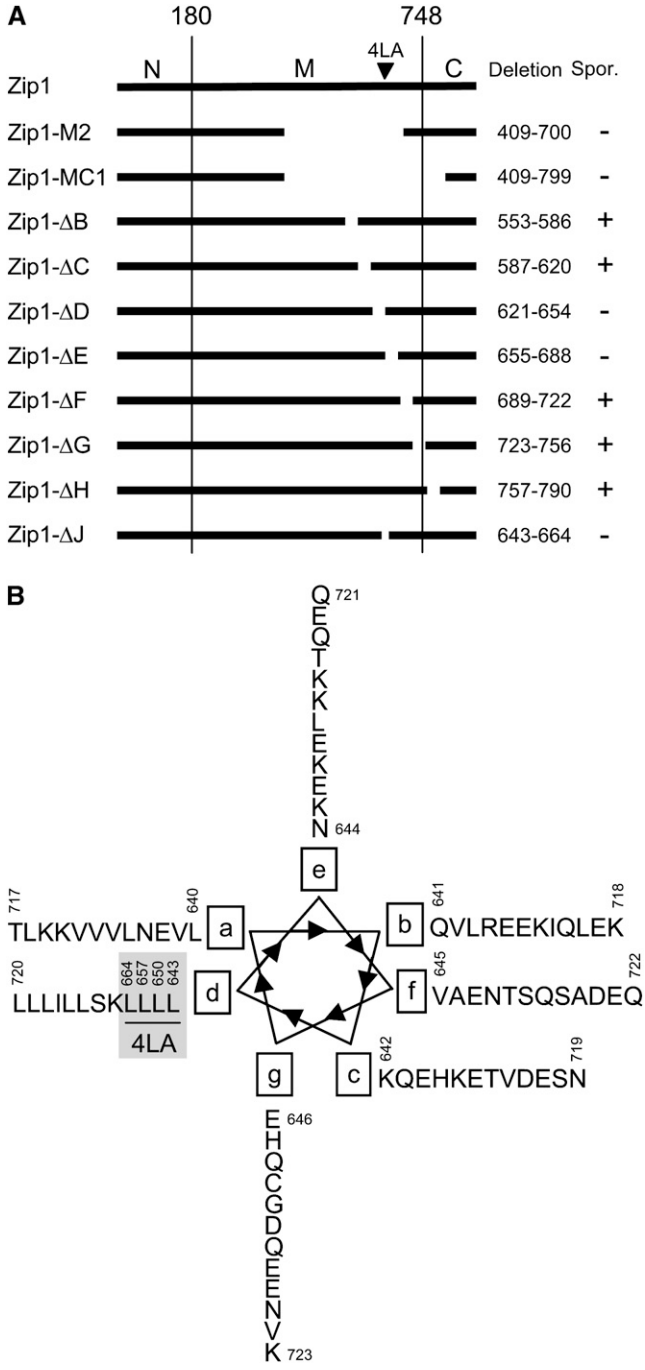

Figure 1.—Structure of Zip1 deletion mutants. (A) Full-length Zip1 protein (875 amino acids) is indicated at the top as a solid line. Vertical lines separate the three domains (N, amino-terminal globular domain; M, middle coiled-coil domain; C, carboxy-terminal globular domain). The arrowhead indicates the position of the 4LA mutation. In-frame deletions are shown by gaps in the solid line, and the deleted amino acid residues are indicated on the right. The ability of each mutant to sporulate (Spor.) in the BR2495 strain background is noted with a + or a − on the far right. Strains used are NMY101–NMY109. Data for Zip1-M2 and Zip1-MC1 are taken from Tung and Roeder (1998). (B) Zip1 residues 640–723 plotted as an α-helical wheel (Landschulz *et al.* 1988; Alber 1992). The four leucines that were changed to alanines in *zip1-4LA* are underlined and shaded.

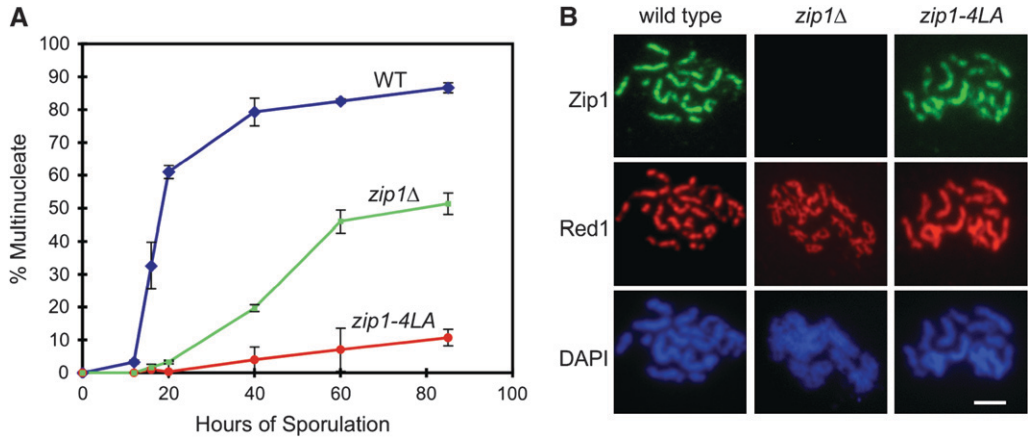

FIGURE 2.—*zip1-4LA* exhibits defects in nuclear division yet has synapsed chromosomes. (A) Nuclear division assay of WT (NMY 274, blue), *zip1*Δ (NMY 364, green), and *zip1-4LA* (NMY363, red) strains in the BR1919-8B diploid background. The graph shows the percentage of cells having completed one or both nuclear divisions as a function of time. (B) Examples of spread nuclei after 18 hr of sporulation. Zip1 (green), Red1 (red), and DAPI (blue) staining are shown for WT, *zip1*Δ, and *zip1-4LA* strains. Bar, 1 μm.

square test, the difference in sporulation between *zip1*Δ and *zip1-4LA* is statistically significant ($P = 0.004$).

To determine if the *zip1-4LA* mutation is dominant, a BR1919-8B diploid heterozygous for *zip1-4LA* was constructed (NMY233). This strain does not arrest, demonstrating that *zip1-4LA* is not dominant for sporulation arrest.

***zip1-4LA* undergoes meiotic cell cycle arrest with synapsed chromosomes:** Nuclear division assays were performed to compare meiotic progression in *zip1-4LA* with wild type and the *zip1*Δ mutant in the BR1919-8B diploid background (Figure 2A). Whole cells were monitored at different time points after the transfer to SPM by staining with the DNA-binding dye, DAPI. In the *zip1*Δ mutant, meiotic division is delayed by ~20 hr compared to wild type, and *zip1-4LA* is almost completely arrested prior to the meiosis I division. Although *zip1-4LA* does not form asci as observed by phase-contrast microscopy, ~10% of *zip1-4LA* nuclei do appear to go through at least the first meiotic division. This observation may be an artifact of the assay (DAPI-stained nuclei appear more fragmented at late time points in all strains, and cells are difficult to categorize). Alternatively, a subpopulation of cells may undergo meiotic division, but nevertheless fail to sporulate.

To determine if chromosomes are synapsed in the *zip1-4LA* mutant, meiotic nuclei were surface spread, stained with antibodies to Zip1 and to the chromosomal core protein Red1 (SMITH and ROEDER 1997), and then visualized by fluorescence microscopy. Synapsis was assessed after 18 hr in sporulation medium, when the number of wild-type cells in pachytene is maximal (Figure 2B). The *zip1-4LA* mutant exhibits fully synapsed chromosomes decorated along their lengths with anti-Zip1 antibodies. In some nuclear spreads, Red1 staining appears more continuous in *zip1-4LA* than in wild type, consistent with previous observations that Red1 accumulates when meiotic progression is delayed (SMITH and ROEDER 1997; CHUA and ROEDER 1998).

Spread nuclei were also examined for the presence of polycomplexes, which are ordered aggregates of SC proteins unassociated with chromosomes (SYM and ROEDER 1995; DONG and ROEDER 2000). Failure to form SC, or a delay in SC formation, leads to the formation of polycomplexes (LOIDL *et al.* 1994; CHUA and ROEDER 1998). These structures are not observed in the *zip1-4LA* mutant, indicating that there is no gross defect or delay in SC assembly. The Zip1-4LA protein is capable of assembling into polycomplexes, as evidenced by the fact that the *spo11 zip1-4LA* double mutant (NMY385) does make polycomplexes (data not shown).

SC assembles with wild-type kinetics in *zip1-4LA*: To investigate further the kinetics of SC assembly, nuclear spreads were analyzed at various time points. *zip1-4LA* cells arrest at pachytene whereas wild-type cells progress out of pachytene. Thus, to compare the kinetics of SC formation in wild-type and *zip1-4LA* strains, the *ndt80* mutation was introduced into both strains. In the *ntd80* background, cells arrest at pachytene (XU *et al.* 1995), thus preventing SC disassembly in *ZIP1* cells.

Both DAPI and Zip1 staining were used to identify spread nuclei. Each spread nucleus was assigned to one of four categories on the basis of the extent of Zip1 staining. Zip1 staining was classified as "no staining" (no Zip1 foci or linear stretches), "dotty" (many individual foci), "dotty linear" (some foci and at least one linear stretch), or "linear" (all staining in linear stretches). No staining, dotty, dotty linear, and linear represent progressively later stages in SC formation. An example of each category is shown in Figure 3A.

The percentage of total spreads in each category of Zip1 staining was plotted as a function of time. The data from one time course are shown in Figure 3B. The *zip1-4LA ndt80* and *ndt80* strains exhibit the same rate of SC assembly. Furthermore, no polycomplexes were observed in either strain at any of the time points examined. Thus, there is no defect or delay in SC formation in the *zip1-4LA* mutant.

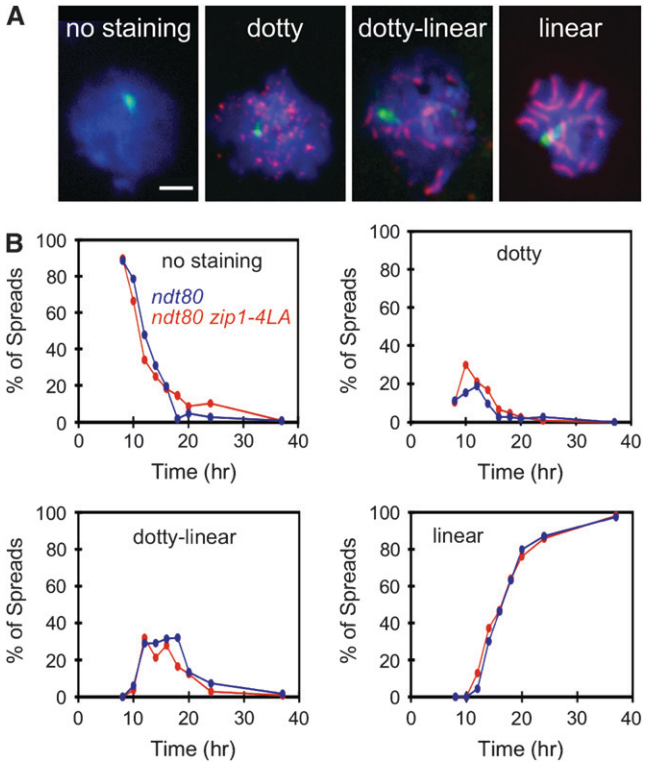

Figure 3.—Kinetics of SC formation. (A) Nuclear spreads were prepared for *ndt80* (NMY539) and *ndt80 zip1-4LA* (NMY533) BR1919-8B diploid strains harvested at nine different time points after the introduction into sporulation medium. Nuclei were stained for Zip1 (red), tubulin (green), and DAPI (blue) and placed into four categories on the basis of Zip1 staining: no staining, dotty (punctate Zip1 foci), dotty linear (Zip1 foci and some elongated stretches of Zip1), and linear (fully elongated Zip1). Bar, 1 μm. (B) Plots of the percentage of *ndt80* (blue) and *ndt80 zip1-4LA* (red) nuclei in each category as a function of time.

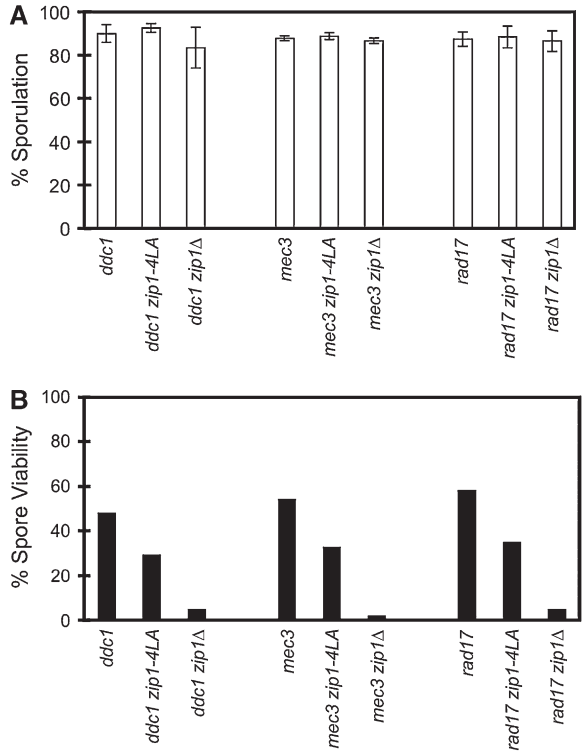

Figure 4.—Sporulation and spore viability. Shown are sporulation (A) and spore viability (B) data for *ddc1* (NMY617), *mec3* (NMY641), and *rad17* (NMY608) single mutants as well as for the same mutants in combination with *zip1-4LA* (NMY611, NMY644, NMY602) or *zip1*Δ (NMY614, NMY647, NMY605). All strains are in the BR1919-8B diploid background. Error bars represent standard deviations.

In a *spo11* mutant, the Zip1 protein localizes only to foci on chromosomes, and these foci correspond to the locations of centromeres (Tsubouchi and Roeder 2005). The Zip1-4LA protein also localizes at or near centromeres in a *spo11* background (data not shown), indicating that this aspect of Zip1 function is not impaired in the *zip1-4LA* mutant.

Bypass of the pachytene checkpoint alleviates the arrest of *zip1-4LA*: In the absence of Spo11, recombination is not initiated, SC is not formed, and the pachytene checkpoint is not activated (reviewed by Bailis and Roeder 2000). To determine if the arrest of *zip1-4LA* can be overcome by preventing checkpoint activation, a *spo11 zip1-4LA* double mutant (NMY385) was assayed for sporulation. The double mutant is able to sporulate similarly to the *spo11* single mutant (NMY422), indicating that arrest of *zip1-4LA* is dependent on some aspect of recombination and/or synapsis. The mere presence of Zip1-4LA protein in the cell is not sufficient to trigger meiotic arrest.

The *DDC1*, *MEC3*, and *RAD17* genes are involved in sensing DNA damage, such as unrepaired double-strand breaks (reviewed by Zhou and Elledge 2000). Each of these genes was knocked out in a *zip1-4LA* background, and the resulting double mutants were assayed for sporulation and spore viability (Figure 4). All of the double mutants are able to sporulate at wild-type levels, indicating that *ddc1*, *mec3*, and *rad17* are each able to bypass the arrest of *zip1-4LA* (Figure 4A). However, in every case, the viability of the double mutant is only ~60% of that of the corresponding *ddc1*, *mec3*, or *rad17* single mutant (Figure 4B). The *ddc1*, *mec3*, and *rad17* mutations by themselves cause a reduction in spore viability compared to wild type (Figure 4B; Lydall *et al.* 1996; Thompson and Stahl 1999; Hong and Roeder 2002).

Mutation of the *SWE1* gene, whose product acts downstream in the checkpoint pathway (Leu and Roeder 1999), was also tested for its ability to bypass *zip1-4LA*. The *swe1* mutation by itself does not affect sporulation or spore viability (Leu and Roeder 1999). The *swe1 zip1-4LA* double mutant is able to sporulate, but at a low level (19.2%) (Figure 5A). The viability of the spores produced is 72.2%, compared to 97.7% in *swe1* and 48.9% in *swe1 zip1*Δ (Figure 5B). Although deletion of *swe1* can partially bypass the meiotic arrest of *zip1-4LA*, the low level of sporulation and the reduction

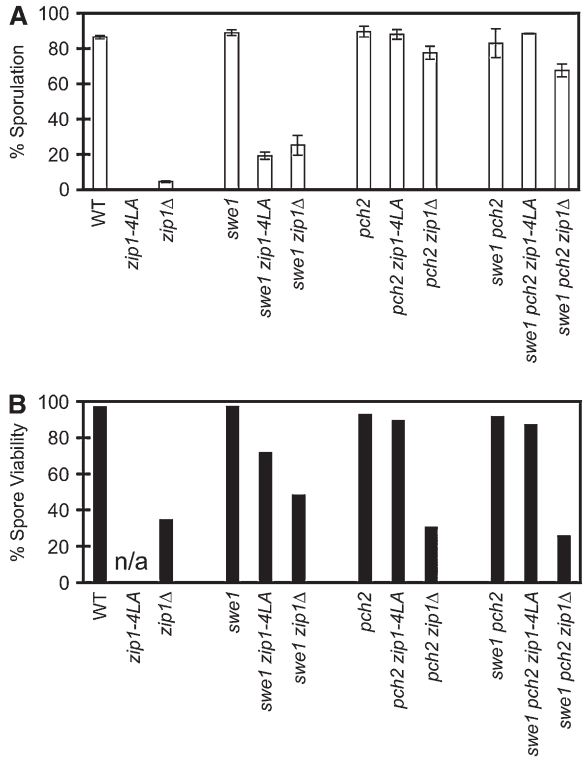

FIGURE 5.—Sporulation and spore viability. Shown are sporulation (A) and spore viability (B) data for wild type (NMY274), *zip1-4LA* (NMY363), *zip1*Δ (NMY364), *swe1* (NMY432), *swe1 zip1-4LA* (NMY340), *swe1 zip1*Δ (NMY345), *pch2* (NMY654), *pch2 zip1-4LA* (NMY661), *pch2 zip1*Δ (NMY664), *swe1 pch2* (NMY565), *swe1 pch2 zip1-4LA* (NMY562), and *swe1 pch2 zip1*Δ (NMY559). All strains are in the BR1919-8B diploid background. Error bars represent standard deviations. n/a, not applicable.

in spore viability in *swe1 zip1-4LA* suggest that bypass of the checkpoint by *swe1* is not sufficient to alleviate all the defects of *zip1-4LA*.

Deletion of the meiosis-specific checkpoint protein Pch2 relieves the pachytene arrest of the *zip1*Δ mutant (SAN-SEGUNDO and ROEDER 1999). To determine if *pch2* can bypass the meiotic arrest of *zip1-4LA*, the *pch2 zip1-4LA* double mutant was assayed for sporulation (Figure 5A) and spore viability (Figure 5B). Sporulation occurs at wild-type levels in the double mutant, indicating that meiotic arrest of *zip1-4LA* is fully bypassed by *pch2*. Furthermore, the viability of the resulting spores is very high (89.8%), similar to (but statistically different from) the viability of spores from the *pch2* single mutant (93.3%) ($P = 5.6 \times 10^{-5}$, chi-square contingency test).

The *swe1 pch2 zip1-4LA* triple mutant is indistinguishable from the *pch2 zip1-4LA* double mutant. Thus *pch2* is epistatic to *swe1*, consistent with the notion that Swe1 acts downstream of Pch2.

***pch2* suppresses the recombination defect of *zip1-4LA*:** The *zip1*Δ mutation reduces, but does not abolish, crossing over (SYM *et al.* 1993; SYM and ROEDER 1994; STORLAZZI *et al.* 1996). To examine the effect of *zip1-4LA* on recombination, crossing over was assessed in a physical assay (GAME *et al.* 1989) using a strain isogenic to the BR1919-8B diploid in which one copy of chromosome III has been circularized. Single crossovers result in a dimeric chromosome III, and three-stranded double crossovers result in a trimeric chromosome III (see MATERIALS AND METHODS). These products can be detected by pulsed-field gel electrophoresis followed by Southern blot analysis.

As shown in Figure 6A, the *zip1*Δ mutant shows a significant delay in the appearance of crossover products, and the overall level of crossing over is reduced substantially compared to wild type, even at late time points (Figure 6A). The *zip1-4LA* mutant shows a delay in crossing over similar to that of *zip1*Δ, but the absolute level of crossovers is higher for *zip1-4LA* than for *zip1*Δ (Figure 6A). The amount of signal in each band was quantified using densitometry. The total signal in the recombinant bands was calculated as a percentage of the total signal in all three bands and then plotted as a function of time (Figure 6D). *zip1-4LA* reaches only ~53% of the wild-type level of crossovers (Figure 6G), even after 70 hr of sporulation. At the same time, crossing over in *zip1*Δ is only 15% of wild type (Figure 6G).

To determine the effect of the *swe1* and *pch2* mutations on recombination in *zip1-4LA*, crossing over was assayed in *swe1 zip1-4LA* and *zip1-4LA pch2* double mutants and compared to the *swe1* and *pch2* single mutants, respectively. The *swe1* and *pch2* single mutants exhibit high levels of spore viability (LEU and ROEDER 1999; SAN-SEGUNDO and ROEDER 1999), suggesting that these mutants undergo wild-type levels of crossing over. The *swe1 zip1-4LA* mutant exhibits a slight improvement in the kinetics of recombinant formation, but the final level of crossover products is still only ~54% of the *ZIP1* control (*i.e.*, the *swe1* single mutant) (Figure 6, B, E, and G). In contrast, crossing over in the *pch2 zip1-4LA* double mutant occurs with normal kinetics and approximately at the *pch2* level (89% of *pch2* at 70 hr). These results are compatible with the spore viability data in Figure 5B. The *swe1 zip1-4LA* double mutant displays reduced spore viability (compared to *swe1* alone), consistent with the observed reduction in crossing over. However, the *pch2 zip1-4LA* double mutant displays nearly wild-type levels of spore viability, as expected for wild-type levels of crossing over.

The *pch2 zip1-4LA* double mutant was also characterized for crossing over by tetrad analysis (Figure 7). Four intervals were assayed, three on chromosome III and one on chromosome VIII. The *pch2 zip1-4LA* strain exhibits levels of crossing over similar to *pch2* in all intervals, consistent with the results of the physical crossover assay. Thus, *zip1-4LA* is proficient in crossing over in a *pch2* background.

Either L657A or L664A is sufficient for meiotic arrest: To determine which of the amino acid substitutions in *zip1-4LA* are required for causing cell cycle arrest,

individual amino acid substitutions L643A, L650A, L657A, and L664A were created. These *ZIP1* mutations were constructed in a centromere-containing plasmid and introduced into a BR2495 strain background in which the chromosomal *ZIP1* gene is deleted. The phenotypes of the four individual leucine-to-alanine substitutions are not identical with respect to sporulation. Both *zip1-L643A* and *zip1-L650A* are able to sporulate well, whereas both *zip1-L657A* and *zip1-L664A* are completely unable to sporulate (data not shown). Therefore, a single leucine-to-alanine substitution at either L657 or L664 is sufficient to cause meiotic cell cycle arrest.

DISCUSSION

***zip1-4LA* is a novel nonnull allele:** The *zip1*Δ mutation leads to a complete failure of SC formation and causes meiotic cell cycle arrest in midmeiotic prophase. In contrast, the *zip1-4LA* mutant makes an apparently normal SC (Figure 2B) with wild-type kinetics (Figure 3B), but cells nevertheless undergo prophase arrest. Given the level of the resolution of fluorescence microscopy, we cannot rule out the possibility of minor disruptions in the SC (*i.e.*, incomplete synapsis) in the *zip1-4LA* mutant. However, even mutants with only modest defects in SC formation exhibit polycomplex formation (*e.g.*, *msh4*; Novak *et al.* 2001), which *zip1-4LA* does not, arguing that both the rate and extent of synapsis are normal in the *zip1-4LA* mutant. We also cannot exclude the possibility that one or a few chromosomes are engaged in nonhomologous synapsis in the *zip1-4LA* mutant. Extensive nonhomologous synapsis (*e.g.*, in *hop2*; Leu *et al.* 1998) leads to delayed synapsis, polycomplex formation, branching networks of chromosomes, and an inability to separate chromosome pairs during spreading; none of these situations applies to the *zip1-4LA* mutant. Note that homologs pair normally in the *zip1* null mutant (Nag *et al.* 1995).

The *zip1-4LA* mutant is similar in phenotype to two deletion mutants characterized previously by Tung and Roeder (1998)—*zip1-M2* and *zip1-MC1*. These mutants also fail to sporulate in the BR2495 background, but they do make SCs. Both of these mutations remove ~300 amino acids from the Zip1 coiled coil (Figure 1A), and they lead to the formation of abnormally narrow SCs, as observed by electron microscopy (Tung and Roeder 1998). It was postulated that the drastic change in the width of the SC is responsible for the arrest in prophase; however, the behavior of the *zip1-4LA* mutant argues against this explanation. Of the many coiled-coil deletion mutants generated in this study, only those that remove the four leucine residues affected by the *zip1-4LA* mutation fail to sporulate. Thus, this region appears to play an especially important role in promoting or regulating cell cycle progression.

Meiotic cell cycle arrest in *zip1-4LA* strains is tighter than in any of the coiled-coil deletion mutants. *zip1-4LA* fails to sporulate in the BR1919-8B background, whereas sporulation occurs at low levels (~2–5%) in mutants in which the 4LA region is deleted, including *zip1-M2*, *zip1-MC1*, *zip1-*Δ*D*, *zip1-*Δ*E*, *zip1-*Δ*J*, and *zip1*Δ. (Sporulation was assessed in strains in which the wild-type *ZIP1* gene was replaced by the *zip1* deletion mutation.) In the SK1 strain background, *zip1-4LA* does sporulate, but the efficiency is reduced compared to the null mutant. The severity of the *zip1-4LA* phenotype, with respect to sporulation, is surprising given the subtle nature of this mutation. The four amino acid changes are all conservative substitutions (leucine to alanine), and they do not affect the predicted ability of the Zip1 protein to form a coiled coil (as determined by Macstripe 2.0, a program based on an algorithm by Lupas *et al.* 1991). Yet the presence of the Zip1-4LA protein has a more deleterious effect on sporulation than the complete absence of Zip1 protein or the presence of Zip1 protein with a dramatically shortened coiled coil.

***zip1-4LA* undergoes checkpoint-induced cell cycle arrest:** A number of observations indicate that meiotic arrest in the *zip1-4LA* mutant is mediated by a cell cycle checkpoint triggered by a defect in meiotic recombination and/or chromosome synapsis. First, the sporulation defect of *zip1-4LA* is suppressed by a *spo11* mutation, which prevents double-strand break formation and the initiation of SC formation (Giroux *et al.* 1989; Loidl *et al.* 1994). Second, the *zip1-4LA* sporulation defect is suppressed by mutations in the *DDC1*, *MEC3*, and *RAD17* genes (Figure 4), whose products are involved in sensing unrepaired double-strand breaks (reviewed by Zhou and Elledge 2000). Finally, the *zip1-4LA* sporulation defect is partially suppressed by deletion of the *SWE1* gene (Figure 5), whose product acts downstream of Ddc1/Med3/Rad17 in the meiotic checkpoint pathway (reviewed by Bailis and Roeder 2000). In every case, however, spore viability in the double mutant (*e.g.*, *ddc1 zip1-4LA* or *swe1 zip1-4LA*) is reduced compared to that in the corresponding single mutant (*e.g.*, *ddc1* or *swe1*), implying that the *zip1-4LA* mutation confers a defect in double-strand break repair and/or chromosome segregation even when the checkpoint is bypassed. Consistent with this interpretation, physical analysis of recombination demonstrates that crossing over occurs at only ~54% of the *swe1* level in the *zip1-4LA swe1* double mutant (Figure 6G).

The sporulation defect of *zip1-4LA* is also suppressed by the absence of the meiosis-specific checkpoint protein Pch2 (San-Segundo and Roeder 1999). In this case, both sporulation and spore viability are restored approximately to *pch2* (*i.e.*, wild-type) levels (Figure 5). Furthermore, meiotic recombination occurs at normal levels in the *pch2 zip1-4LA* double mutant, as evidenced in both genetic and physical assays (Figures 6 and 7). The behavior of the *pch2 zip1-4LA* double mutant provides

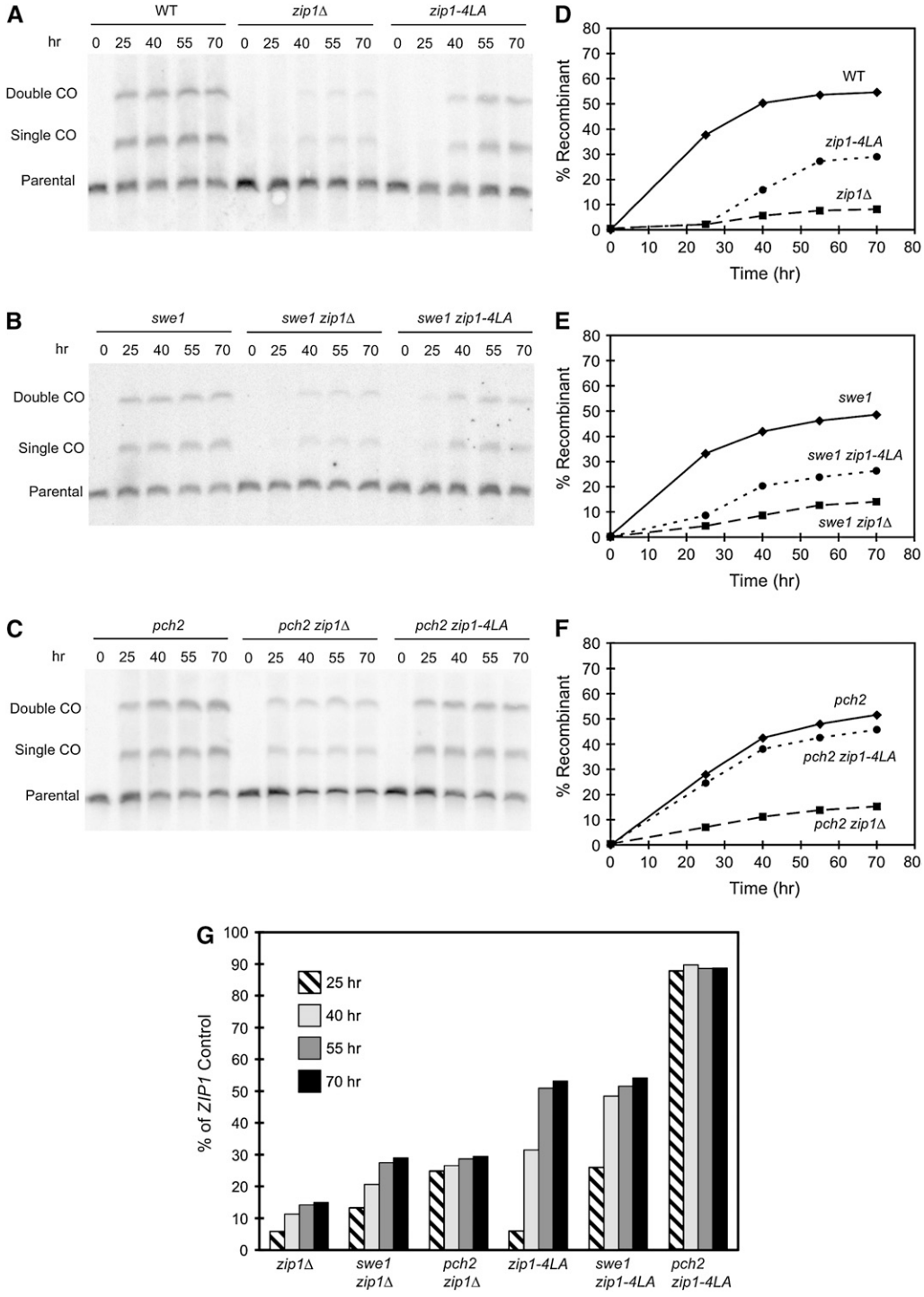

FIGURE 6.—Physical assay of recombination. This assay measures crossing over along the entire length of chromosome III for the entire cell population. At various time points, cells were collected from SPM and chromosomes were subjected to pulsed-field electrophoresis followed by Southern blot analysis probing for chromosome III (A–C). A single crossover between the parental circular and linear chromosome III homologs is detected as a band that is twice the molecular weight of the parental linear chromosome III. A (three-stranded) double crossover is detected as a band that is three times the molecular weight. The parental circular chromosome does not enter the gel and is therefore not detected (see MATERIALS AND METHODS). The bottom band represents parental linear chromosome III and the middle and top bands represent single-crossover (single CO) and double-crossover (double CO) products, respectively. (A) Assay of wild type (NMY268), *zip1*Δ (NMY270), and *zip1-4LA* (NMY272) strains; (B) the same assay performed in a *swe1* background (NMY471, NMY473, NMY472); (C) the same assay performed in a *pch2* background (NMY671, NMY672, NMY673). (D–F) For each blot on the left, the total signal in the two recombinant bands was calculated as a percentage of the total signal in all three bands and plotted as a function of time. (G) Histograms of the amount of crossing over of *zip1*Δ and *zip1-4LA* strains as a percentage of the corresponding *ZIP1* control strains. For example, the bars labeled *swe1 zip1*Δ represent the level of crossing over in the *swe1 zip1*Δ strain expressed as a percentage of the *swe1 ZIP1* control analyzed in the same experiment. Comparisons were made at all four meiotic time points (25, 40, 55, and 70 hr).

additional evidence that prophase arrest in *zip1-4LA* strains is mediated by a meiotic checkpoint and suggests a special relationship between Pch2 and Zip1, as discussed further below.

Why does the *zip1-4LA* mutant arrest in prophase? What is the nature of the defect that triggers cell cycle arrest in *zip1-4LA* strains? There are at least three possibilities. First, arrest might be triggered by unrepaired double-strand breaks or some other recombination intermediate. Second, the *zip1-4LA* mutant might be defective in SC disassembly, and cell cycle progression might be blocked as long as the SC persists. Third, the checkpoint might be activated by an aberration in SC structure caused by the *zip1-4LA* mutation.

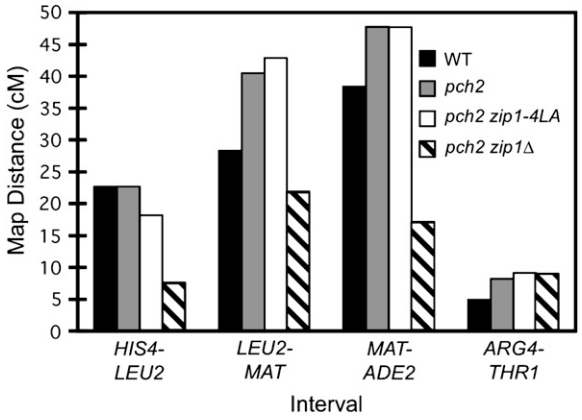

FIGURE 7.—Tetrad analysis of *pch2 zip1-4LA* strains. Shown is the map distance (centimorgans) in three intervals on chromosome III and in one interval on chromosome VIII for wild-type (NMY650), *pch2* (NMY654), *pch2 zip1-4LA* (NMY661), and *pch2 zip1*Δ (NMY664) strains in the BR1919-8B diploid background. Using the *G*-test of homogeneity, there is no statistically significant difference between map distances in *pch2* and *pch2 zip1-4LA* for any interval: $P = 0.460$ for *HIS4-LEU2*; $P = 0.617$ for *LEU2-MAT*; $P = 0.843$ for *MAT-ADE2*; $P = 0.884$ for *ARG4-THR1*.

A physical assay demonstrates that the production of crossover products is delayed, and the final level of crossover products is reduced, in the *zip1-4LA* single mutant (Figure 6, A and B). This observation raises the possibility that the checkpoint is activated by recombination intermediates, such as unrepaired double-strand breaks. Previous studies suggested that the Zip1 protein plays a role in recombination (STORLAZZI *et al.* 1996), and this function may be impaired by the *zip1-4LA* mutation. Arguing against this possibility, however, is the observation that the *pch2 zip1-4LA* mutant undergoes normal levels of crossing over with the same kinetics as wild type (Figure 6, C, F, and G). This result suggests that *zip1-4LA* is not deficient in recombination *per se* and argues that the decrease in recombination is an indirect consequence of cell cycle arrest. The mutant might arrest at a stage in the cell cycle prior to the point at which recombination intermediates are normally resolved.

In wild type, the SC disassembles prior to formation of the metaphase I spindle (PADMORE *et al.* 1991). Perhaps SC containing the Zip1-4LA protein is unable to disassemble, and persistence of the SC is the cause (rather than the consequence) of cell cycle arrest at pachytene. Attempting chromosome segregation with some or all pairs of homologs still held together by SC would lead to defects in chromosome segregation and might account for the reduced spore viability observed in the *swe1 zip1-4LA* double mutant. To investigate this possibility, meiosis I nuclei from *swe1* and *swe1 zip1-4LA* cells were examined for staining with Zip1 antibodies. None of the nuclei with spindles (identified by tubulin staining) exhibited any Zip1 staining (data not shown), arguing against a defect in SC disassembly. Meiosis I nuclei from *zip1-4LA pch2* cells also do not exhibit Zip1 staining, consistent with the high spore viability observed in this strain.

The presence of the Zip1-4LA protein might alter the structure of the SC, and this aberration may be detected by a surveillance mechanism that monitors SC morphology. Perhaps the region defined by the *zip1-4LA* mutation is involved in interacting with another protein, possibly another component of the SC central region. In mutants in which the *zip1-4LA* region is deleted, this protein might be absent from the SC, whereas this protein might be present in an aberrant configuration in the *zip1-4LA* mutant. This difference might explain the difference in the severity of cell cycle arrest in the deletion mutants *vs. zip1-4LA*.

The observation that *zip1-L657A* and *zip1-L664A* are completely unable to sporulate, while *zip1-L643A* and *zip1-L650A* are able to sporulate well, demonstrates that the phenotype of *zip1-4LA* is specific to certain residues in the 4LA region. Equilibrium and kinetic circular dichroism studies of the Gcn4 leucine zipper have indicated that the third and fourth heptad repeats in the zipper are the heptads that drive leucine zipper formation (ZITZEWITZ *et al.* 2000). Thus, the observation that L657A and L664A (in the third and fourth heptads) cause a sporulation defect suggests that the *zip1-4LA* mutation perturbs the Zip1 dimer interaction. Although the Zip1 dimer might be perturbed locally in the 4LA region, it is unlikely that the Zip1-4LA protein completely fails to dimerize because the four heptads affected by the *zip1-4LA* mutation are embedded in a very long coiled-coil region consisting of ~80 heptad repeats. Furthermore, a Zip1 protein that failed to dimerize would almost certainly not support SC formation.

A previous study (DONG and ROEDER 2000) showed that two Zip1 dimers lie head to head to span the width of the SC, with the carboxy termini of Zip1 associated with lateral elements and the amino termini located near the middle of the central region. On the basis of the analysis of Zip1 deletion mutants (TUNG and ROEDER 1998), it was suggested that Zip1 dimers attached to opposing lateral elements overlap in the amino-terminal portion of the coiled coil. The Zip1-4LA mutation is located close to the carboxy terminus of the Zip1 coiled coil and therefore is not expected to affect the interaction between Zip1 dimers.

***zip1-4LA* may trigger a Pch2-dependent synapsis checkpoint:** The *PCH2* gene was originally identified in a screen for mutations that allow the *zip1*Δ mutant to sporulate (SAN-SEGUNDO and ROEDER 1999). Unlike the *ddc1/mec3/rad17* mutations, *pch2* does not fully suppress the sporulation defect of mutants defective in the enzymology of recombination, such as *dmc1* or *hop2* (SAN-SEGUNDO and ROEDER 1999; ZIERHUT *et al.* 2004; HOCHWAGEN *et al.* 2005). Thus, Pch2 may monitor processes or structures distinct from recombination.

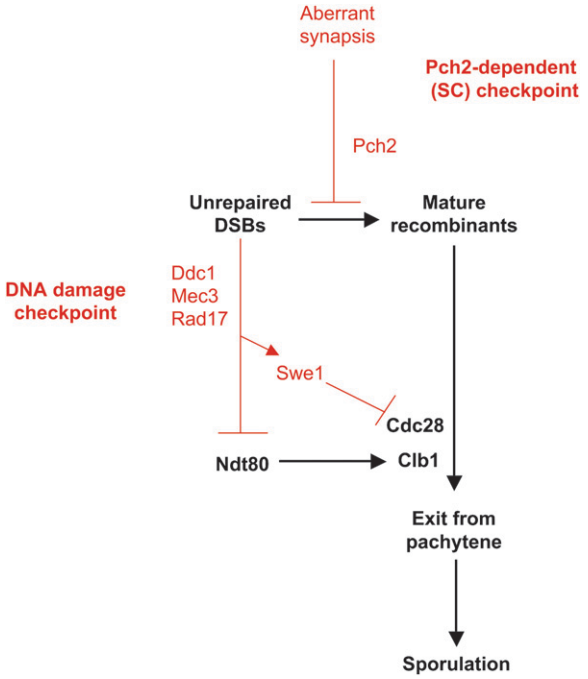

FIGURE 8.—Model of the relationship between SC and DNA damage checkpoints. Proteins and events involved in normal cell cycle progression are indicated in black; proteins and events involved in checkpoint-induced cell cycle arrest are depicted in red. Pch2 might function to ensure proper coupling between SC morphogenesis and meiotic recombination. A signal from aberrant SC could signal Pch2 to inhibit late steps in recombination, either by preventing the completion of recombination or by blocking progression to the stage in the cell cycle when recombination normally is completed. Accumulation of recombination intermediates would then trigger the DNA damage checkpoint, dependent on Ddc1/Mec3/Rad17. WU and BURGESS (2006) have shown that almost all of the spores produced by a *pch2 rad17* double mutant are inviable, suggesting that Pch2 and/or Rad17 have additional unknown functions.

Recently, WU and BURGESS (2006) showed that the Pch2 and Rad17 proteins act independently to negatively regulate meiotic cell cycle progression. In addition, they presented evidence that the Zip1 protein is required for Pch2-mediated inhibition of cell cycle progression. They argued that the presence of incomplete or aberrant SC activates a synapsis checkpoint whose function depends on Pch2. Consistent with this hypothesis, Pch2 orthologs are present in organisms known to make SCs, but absent from eukaryotes in which meiotic chromosomes do not undergo synapsis (WU and BURGESS 2006).

Compelling evidence that Pch2 acts in a checkpoint that monitors synapsis comes from studies in *C. elegans*, in which SC assembly occurs independently of recombination (BHALLA and DERNBURG 2005). In this organism, chromosome pairing and synapsis initiate at *cis*-acting loci called pairing centers (MACQUEEN *et al.* 2005); these centers are present at one end of each chromosome pair (WICKY and ROSS 1996). BHALLA and DERNBURG (2005) showed that in strains hemizygous for the X chromosome pairing center, the X chromosomes often fail to synapse and consequently fail to cross over. Furthermore, they observed a correlation between the frequency of asynaptic X chromosomes and the frequency of meiotic cells undergoing apoptosis. This programmed cell death is Pch2 dependent, suggesting that Pch2 plays a role in preventing cells with asynaptic chromosomes from completing gametogenesis. The Pch2-dependent cell death that occurs in pairing-center hemizygotes is independent of genes whose products act in the meiotic recombination checkpoint pathway.

Model for Pch2-mediated arrest of *zip1-4LA*: The recent evidence that Pch2 acts in an SC checkpoint pathway supports our hypothesis that cell cycle arrest in *zip-4LA* is due to formation of an SC that is recognized as aberrant. But if SC structure is the primary defect in *zip1-4LA*, then why is the sporulation defect alleviated by the *ddc1/mec3/rad17* family of mutations? One possibility is that Pch2 functions to ensure the proper coupling between SC morphogenesis and meiotic recombination (Figure 8). In response to the *zip1-4LA*-induced perturbation in SC structure, Pch2 may block late steps in recombination, either by inhibiting recombination *per se* or by blocking cell cycle progression. The accumulation of recombination intermediates would then trigger the recombination checkpoint, mediated by the Ddc1/Mec3/Rad17 proteins in conjunction with other players. According to this model, Pch2 acts upstream of Ddc1/Mec3/Rad17 in the checkpoint pathway, and the defect in recombination is a consequence of Pch2's response to the perturbation in SC structure.

We thank previous and current members of the Roeder lab for helpful comments on the manuscript and for their support and encouragement. N.M. thanks H. Tsubouchi for many helpful discussions and for technical support. Oligonucleotide synthesis and DNA sequencing were performed by the W. M. Keck Foundation Biotechnology Resource Laboratory at Yale University. This work was supported by National Institutes of Health grant GM28904 (to G.S.R.) and by the Howard Hughes Medical Institute.

LITERATURE CITED

AGARWAL, S., and G. S. ROEDER, 2000 Zip3 provides a link between recombination enzymes and synaptonemal complex proteins. Cell **102:** 245–255.

ALANI, E., L. CAO and N. KLECKNER, 1987 A method for gene disruption that allows repeated use of *URA3* selection in the construction of multiply disrupted yeast strains. Genetics **116:** 541–545.

ALBER, T., 1992 Structure of the leucine zipper. Curr. Opin. Genet. Dev. **2:** 205–210.

ALLERS, T., and M. LICHTEN, 2001 Differential timing and control of noncrossover and crossover recombination during meiosis. Cell **106:** 47–57.

BAILIS, J. M., and G. S. ROEDER, 2000 The pachytene checkpoint. Trends Genet. **16:** 395–403.

BENJAMIN, K. R., C. ZHANG, K. M. SHOKAT and I. HERSKOWITZ, 2003 Control of landmark events in meiosis by the CDK Cdc28 and the meiosis-specific kinase Ime2. Genes Dev. **17:** 1524–1539.

BHALLA, N., and A. F. DERNBURG, 2005 A conserved checkpoint monitors meiotic chromosome synapsis in *Caenorhabditis elegans*. Science **310:** 1683–1686.

BISHOP, D. K., D. PARK, L. XU and N. KLECKNER, 1992 *DMC1*: a meiosis-specific yeast homolog of E. coli *recA* required for

recombination, synaptonemal complex formation, and cell cycle progression. Cell **69:** 439–456.

Boeke, J. D., F. Lacroute and G. R. Fink, 1984 A positive selection for mutants lacking orotidine-5′-phosphate decarboxylase activity in yeast: 5-fluoro-orotic acid resistance. Mol. Gen. Genet. **197:** 345–346.

Booher, R. N., R. J. Deshaies and M. W. Kirschner, 1993 Properties of *Saccharomyces cerevisiae* wee1 and its differential regulation of $p34^{CDC28}$ in response to G_1 and G_2 cyclins. EMBO J. **12:** 3417–3426.

Chu, S., and I. Herskowitz, 1998 Gametogenesis in yeast is regulated by a transcriptional cascade dependent on Ndt80. Mol. Cell **1:** 685–696.

Chua, P. R., and G. S. Roeder, 1998 Zip2, a meiosis-specific protein required for the initiation of chromosome synapsis. Cell **93:** 349–359.

Dong, H., and G. S. Roeder, 2000 Organization of the yeast Zip1 protein within the central region of the synaptonemal complex. J. Cell Biol. **148:** 417–426.

Dresser, M. E., and C. N. Giroux, 1988 Meiotic chromosome behavior in spread preparations of yeast. J. Cell Biol. **106:** 567–578.

Engebrecht, J., and G. S. Roeder, 1989 Yeast *mer1* mutants display reduced levels of meiotic recombination. Genetics **121:** 237–247.

Esposito, R. E., M. Dresser and M. Breitenbach, 1991 Identifying sporulation genes, visualizing synaptonemal complexes, and large-scale spore and spore wall purification. Methods Enzymol. **194:** 110–131.

Fung, J. C., B. Rockmill, M. Odell and G. S. Roeder, 2004 Imposition of crossover interference through the nonrandom distribution of synapsis initiation complexes. Cell **116:** 795–802.

Game, J. C., K. C. Sitney, V. E. Cook and R. K. Mortimer, 1989 Use of a ring chromosome and pulsed-field gels to study interhomolog recombination, double-strand DNA breaks and sister-chromatid exchange in yeast. Genetics **123:** 695–713.

Giroux, C. N., M. E. Dresser and H. F. Tiano, 1989 Genetic control of chromosome synapsis in yeast meiosis. Genome **31:** 88–94.

Goldstein, A. L., and J. H. McCusker, 1999 Three new dominant drug resistance cassettes for gene disruption in Saccharomyces cerevisiae. Yeast **15:** 1541–1553.

Hepworth, S. R., H. Friesen and J. Segall, 1998 *NDT80* and the meiotic recombination checkpoint regulate expression of middle sporulation-specific genes in *Saccharomyces cerevisiae*. Mol. Cell. Biol. **18:** 5750–5761.

Ho, S. N., H. D. Hunt, R. M. Horton, J. K. Pullen and L. R. Pease, 1989 Site-directed mutagenesis by overlap extension using the polymerase chain reaction. Gene **77:** 51–59.

Hochwagen, A., W.-H. Tham, G. A. Brar and A. Amon, 2005 The FK506 binding protein Fpr3 counteracts protein phosphatase 1 to maintain meiotic recombination checkpoint activity. Cell **122:** 861–873.

Hong, E. E., and G. S. Roeder, 2002 A role for Ddc1 in signaling meiotic double-strand breaks at the pachytene checkpoint. Genes Dev. **16:** 363–376.

Keeney, S., 2001 Mechanism and control of meiotic recombination initiation. Curr. Top. Dev. Biol. **52:** 1–53.

Landschulz, W. H., P. F. Johnson and S. L. McKnight, 1988 The leucine zipper: a hypothetical structure common to a new class of DNA binding proteins. Science **240:** 1759–1764.

Leu, J.-Y., and G. S. Roeder, 1999 The pachytene checkpoint in *S. cerevisiae* depends on Swe1-mediated phosphorylation of the cyclin-dependent kinase Cdc28. Mol. Cell **4:** 805–814.

Leu, J.-Y., P. R. Chua and G. S. Roeder, 1998 The meiosis-specific Hop2 protein of *S. cerevisiae* ensures synapsis between homologous chromosomes. Cell **94:** 375–386.

Loidl, J., F. Klein and H. Scherthan, 1994 Homologous pairing is reduced but not abolished in asynaptic mutants of yeast. J. Cell Biol. **125:** 1191–1200.

Longhese, M. P., R. Fraschini, P. Plevani and G. Lucchini, 1996 Yeast *pip3/mec3* mutants fail to delay entry into S phase and to slow DNA replication in response to DNA damage, and they define a functional link between Mec3 and DNA primase. Mol. Cell. Biol. **16:** 3235–3244.

Lupas, A., M. V. Dyke and J. Stock, 1991 Predicting coiled-coils from protein sequences. Science **252:** 1162–1164.

Lydall, D., and T. Weinert, 1997 G2/M checkpoint genes of *Saccharomyces cerevisiae*: further evidence for roles in DNA replication and/or repair. Mol. Gen. Genet. **256:** 638–651.

Lydall, D., Y. Nikolsky, D. K. Bishop and T. Weinert, 1996 A meiotic recombination checkpoint controlled by mitotic checkpoint genes. Nature **383:** 840–843.

MacQueen, A. J., C. M. Phillips, N. Bhalla, P. Weiser, A. M. Villeneuve *et al.*, 2005 Chromosome sites play dual roles to establish homologous synapsis during meiosis in *C. elegans*. Cell **123:** 1037–1050.

Nag, D. K., H. Scherthan, B. Rockmill, J. Bhargava and G. S. Roeder, 1995 Heteroduplex DNA formation and homolog pairing in yeast meiotic mutants. Genetics **141:** 75–86.

Novak, J. E., P. Ross-Macdonald and G. S. Roeder, 2001 The budding yeast Msh4 protein functions in chromosome synapsis and the regulation of crossover distribution. Genetics **158:** 1013–1025.

Oldenburg, K. R., K. T. Vo, S. Michaelis and C. Paddon, 1997 Recombination-mediated PCR-directed plasmid construction in vivo in yeast. Nucleic Acids Res. **25:** 451–452.

Padmore, R., L. Cao and N. Kleckner, 1991 Temporal comparison of recombination and synaptonemal complex formation during meiosis in *S. cerevisiae*. Cell **66:** 1239–1256.

Rockmill, B., and G. S. Roeder, 1990 Meiosis in asynaptic yeast. Genetics **126:** 563–574.

Rockmill, B., M. Sym, H. Scherthan and G. S. Roeder, 1995 Roles for two RecA homologs in promoting meiotic chromosome synapsis. Genes Dev. **9:** 2684–2695.

Roeder, G. S., 1997 Meiotic chromosomes: it takes two to tango. Genes Dev. **11:** 2600–2621.

San-Segundo, P., and G. S. Roeder, 1999 Pch2 links chromatin silencing to meiotic checkpoint control. Cell **97:** 313–324.

Schwacha, A., and N. Kleckner, 1994 Identification of joint molecules that form frequently between homologs but rarely between sister chromatids during yeast meiosis. Cell **76:** 51–63.

Sherman, F., G. R. Fink and J. B. Hicks, 1986 *Methods in Yeast Genetics: A Laboratory Manual*. Cold Spring Harbor Laboratory Press, Cold Spring Harbor, NY.

Shuster, E. O., and B. Byers, 1989 Pachytene arrest and other meiotic effects of the start mutations in *Saccharomyces cerevisiae*. Genetics **123:** 29–43.

Sikorski, R., and P. Hieter, 1989 A system of shuttle vectors and yeast host strains designed for efficient manipulation of DNA in *Saccharomyces cerevisiae*. Genetics **122:** 19–27.

Smith, A. V., and G. S. Roeder, 1997 The yeast Red1 protein localizes to the cores of meiotic chromosomes. J. Cell Biol. **136:** 957–967.

Sokal, R. R., and F. J. Rohlf, 1995 *Biometry*. W. H. Freeman, San Francisco/New York.

Storlazzi, A., L. Xu, A. Schwacha and N. Kleckner, 1996 Synaptonemal complex (SC) component Zip1 plays a role in meiotic recombination independent of SC polymerization along the chromosomes. Proc. Natl. Acad. Sci. USA **93:** 9043–9048.

Sym, M., and G. S. Roeder, 1994 Crossover interference is abolished in the absence of a synaptonemal complex protein. Cell **79:** 283–292.

Sym, M., and G. S. Roeder, 1995 Zip1-induced changes in synaptonemal complex structure and polycomplex assembly. J. Cell Biol. **128:** 455–466.

Sym, M., J. Engebrecht and G. S. Roeder, 1993 Zip1 is a synaptonemal complex protein required for meiotic chromosome synapsis. Cell **72:** 365–378.

Thompson, D. A., and F. W. Stahl, 1999 Genetic control of recombination partner preference in yeast meiosis: isolation and characterization of mutants elevated for meiotic unequal sister-chromatid recombination. Genetics **153:** 621–641.

Tsubouchi, T., and G. S. Roeder, 2005 A synaptonemal complex protein promotes homology-independent centromere coupling. Science **308:** 870–873.

Tsubouchi, T., H. Zhao and G. S. Roeder, 2006 The meiosis-specific Zip4 protein regulates crossover distribution by promoting synaptonemal complex formation together with Zip2. Dev. Cell **10:** 809–819.

Tung, K.-S., and G. S. Roeder, 1998 Meiotic chromosome morphology and behavior in *zip1* mutants of *Saccharomyces cerevisiae*. Genetics **149:** 817–832.

Tung, K.-S., E. Hong and G. S. Roeder, 2000 The pachytene checkpoint prevents accumulation and phosphorylation of the

meiosis-specific transcription factor Ndt80. Proc. Natl. Acad. Sci. USA **97:** 12187–12192.

Wach, A., A. Brachat, R. Pohlmann and P. Philippsen, 1994 New heterologous modules for classical or PCR-based gene disruptions in *Saccharomyces cerevisiae*. Yeast **10:** 1793–1808.

Wang, H., S. Frackman, J. Kowalisyn, R. E. Esposito and R. Elder, 1987 Developmental regulation of *SPO13*, a gene required for separation of homologous chromosomes at meiosis I. Mol. Cell. Biol. **7:** 1425–1435.

Wicky, C., and A. M. Ross, 1996 The role of chromosome ends during meiosis in *Caenorhabditis elegans*. BioEssays **18:** 447–452.

Wu, H.-Y., and S. M. Burgess, 2006 Meiotic chromosome metabolism is monitored by two distinct prophase checkpoints in budding yeast. Curr. Biol. **16:** 2473–2479.

Xu, L., M. Ajimura, R. Padmore, C. Klein and N. Kleckner, 1995 *NDT80*, a meiosis-specific gene required for exit from pachytene in *Saccharomyces cerevisiae*. Mol. Cell. Biol. **15:** 6572–6581.

Xu, L., B. M. Weiner and N. Kleckner, 1997 Meiotic cells monitor the status of the interhomolog recombination complex. Genes Dev. **11:** 106–118.

Zhou, B.-B. S., and S. J. Elledge, 2000 The DNA damage response: putting checkpoints in perspective. Nature **408:** 433–439.

Zickler, D., and N. Kleckner, 1999 Meiotic chromosomes: integrating structure and function. Annu. Rev. Genet. **33:** 603–754.

Zierhut, C., M. Berlinger, C. Rupp, A. Shinohara and F. Klein, 2004 Mnd1 is required for meiotic interhomolog repair. Curr. Biol. **14:** 752–762.

Zitzewitz, J. A., B. Ibarra-Molero, D. R. Fishel, K. L. Terry and C. R. Matthews, 2000 Preformed secondary structure drives the association reaction of GCN4-p1, a model coiled-coil system. J. Mol. Biol. **296:** 1105–1116.

Communicating editor: G. R. Smith